Inferring Congestion in The Internet via Moment-Based Estimators

Sara Alouf

Supervisor : Philippe Nain
Team : Mistral

Internship Report
DEA RSD, 1999

Contents

Chapter 1

Introduction

The huge expansion of the Internet coupled to the emergence of new (in particular, multimedia) applications pose challenging problems in terms of performance and control of the network. These include the design of efficient congestion control and recovery mechanisms, and the ability of the network to offer a good Quality of Service (QoS) to the users. In the current Internet, there is a single class best effort service which does not promise anything to the users in terms of performance guarantees. The forthcoming deployment in the Internet of differentiated services (known as *diffserv* [1]) will be a first (long awaited) step towards the support of various types of applications and business requirements. It is however doubtful that Diffserv – that will mark each packet to receive a particular forwarding treatement, or per-hop behavior, at each network node – or the RED mechanism for congestion avoidance in gateways [6] alone will solve all QoS issues raised by real-time applications. Diffserv and RED are two instances of a general approach that aims at adding more intelligence in the *network*. A more ambitious component of this approach is captured in the concept of *active networking* [20] that aims at exploiting mobile code and programmable infrastructure to provide rapid and specialized service introduction.

Another and complementary approach for providing QoS guarantees is to add intelligence in the *applications*. This idea is to provide applications with enough knowledge on the network so that they can use this information to adapt their transmission rates to current network conditions. Since it is impossible to monitor every link on the Internet, network internal static (e.g. bandwith of a link) and dynamic (e.g. available bandwith on a path) characteristics have to be estimated from end-to-end measurements when available, or only from measurements performed by the sender based on feedback information (e.g. packet losses) delivered by the network (e.g. RTCP feedback). Estimation schemes based on the *packet pair* technique [8, Ch. 4] have been

[1] http://www.ietf.org/html.charters/diffserv-charter.html

devised for estimating bottleneck bandwidths [1, 4, 12] and the available bandwith for a path between two hosts on the Internet [4, 7, 9, 12]. In a different context, estimating traffic parameters in queueing systems with local information have been devised for estimating the traffic intensity on the entering node of the network for the Call Acceptance Controller (CAC) in ATM networks [15].

Measurements may also be used to estimate some network internal characteristics via *inference models*. The inference methodology has been applied to estimate loss rates on internal links [3], the optimal amount of redundant information to be used in an adaptive FEC-based error control algorithm for Internet telephony [2], traffic matrices from measurements of aggregate flows taken in a number of points in a network [18, 19], the internal structure of a multicast tree [13] and loss rate and delay distribution [16].

In this work, we develop simple inference models, based on a finite capacity single server queue, for estimating the *buffer size* and the *intensity of cross traffic* at the bottleneck link of a path between two hosts. Several pairs of *moment-based* estimators are proposed to estimate these two quantities both in the case when end-to-end measurements are available and when only measurements at the sender are available. The performance (speed of convergence, variance, robustness to statistical assumptions and to network topology, etc.) of these estimators are then evaluated and classified through simulations developped in *ns* [11].

Chapter 2

Why inference models?

Often direct estimation of Internet performance parameters leads to estimators with a large variance, which is unsuitable for real-time applications. These applications suffer a degradation in quality, whenever losses exceed a certain percentage, jitter delays become important and delays get large. When an estimator has a large variance, the rate of the real-time application mismatches the available capacity in the network. This results in a quality of service different from the expected one.

Estimation of network characteristics and performance metrics via inference based models is an emerging area of research. For the first time this year an entire session was devoted to this topic during the annual INFOCOM conference[1]. For us, an inference model is an *a priori* mathematical model of a physical system (a route in a network in our case) that will allow us to estimate non-observable characteristics of the system from the available data set (e.g. end-to-end measurements in the network setting).

As usual in estimation theory, a "good" estimator must capture several desirable properties; it must preferably be unbiased, efficient, consistent (see Section 5.4 for a refresher on these notions) but also in our context easy to implement without interfering on the performance of the network (no latency added, etc.).

As an example, we will discuss the inference models used in [13] and [16]. In [13], end-to-end measurements were used in inferring the internal structure of a multicast distribution tree. In a first step, correlations of loss patterns across the receiver set were noted and how the network perturbs the fine-grained timing structure of the packets sent from the source was measured. This led in a second step to the determination of both underlying multicast tree structure as well as the bottleneck bandwidths. In [16], an algorithm

[1] *IEEE INFOCOM'99* Conf., New York, March 23-25, 1999.

that collects a histogram of the occupancy of a single-server queue at packet arrival times was outlined. This algorithm also infers the loss rate and delay distribution from such measurements.

Chapter 3

The M+M/M/1/K queue

Part of the material presented in this chapter is due to P. Nain and D. Towsley.

3.1 The model

We model an Internet connection by a single queue representing its bottleneck. The buffer is finite with room for K customers, $K-1$ customers in the waiting room and one customer in the server. The incoming traffic at the bottleneck is modelled as two independent Poisson sources: the probe traffic generated by a foreground source with rate γ, and the cross traffic generated by a background source with rate λ. Service times are assumed to be i.i.d. random variables with exponential distribution with mean $1/\mu$, further independent of the arrival processes (see Figure 3.1).

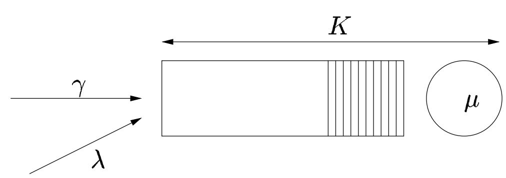

Figure 3.1: The model

The exponential assumption models the fact that the packets length is variable, some packets being small like the acknowledgments of TCP traffic, others being ten times larger. The traffic intensity is defined as

$$\rho = \frac{\lambda+\gamma}{\mu}. \tag{3.1}$$

We are interested in the behavior of the system from the perspective of the foreground customers. This includes stationary measures such as expected delay, loss probability, server occupation and a number of additional statistics associated with the foreground loss process, namely, the probability of two consecutive losses and the probability of two consecutive successes.

Let $\{Q_n\}_{n=1}^{\infty}$ be the process of the number of packets in the buffer at time of the n-th arrival from foreground source, and let $Q = \lim_{n\to\infty} Q_n$[1]. The distribution of Q is

$$\pi_i \quad = \quad P(Q = i).$$

It is known that [10]

$$\pi_i \quad = \quad \frac{(1-\rho)\rho^i}{1-\rho^{K+1}}, \qquad i = 0, 1, \ldots, K. \tag{3.2}$$

3.2 The loss probability

We focus here on the loss process. We define $X_n = \mathbf{1}\{Q_n = K\}$ and $X = \lim_{n\to\infty} X_n$. A customer is lost whenever it arrives to a full buffer. In other words, customer n is lost whenever $X_n = 1$ and is not lost otherwise. Let $\{a_n\}_{n=1}^{\infty}$ and $\{d_n\}_{n=1}^{\infty}$ be the arrival times to the system and the departure times from the system, respectively, of the n-th foreground customer, $n = 1, 2, \ldots$. When a packet is lost, it never reaches the destination. We shall assume that $d_n = \infty$ if $X_n = 1$.

The probability that a foreground customer arrives to find the system full, and is lost, is

$$\begin{aligned} P_L \quad &:= \quad P(X = 1) \\ &= \quad P(Q = K) \\ &= \quad \pi_K \; = \; \frac{(1-\rho)\,\rho^K}{1-\rho^{K+1}}. \end{aligned} \tag{3.3}$$

Observe that the expression for P_L can be used to give the following expression for K in terms of ρ and P_L,

$$K \quad = \quad \frac{1}{\log\rho} \cdot \log\left(\frac{P_L}{1-\rho\,(1-P_L)}\right). \tag{3.4}$$

[1]A word on the notation. Let $\{Z_n\}_n$ be a sequence of random variables taking values in $[0,\infty)$. Assume that $\lim_{n\to\infty} P[Z_n \le x]$ exists for all $x \ge 0$. Then $Z = \lim_{n\to\infty} Z_n$ designates any random variable such that $P[Z \le x] = \lim_{n\to\infty} P[Z_n \le x]$

3.3 The server occupation

The second metric of interest to us is the occupation U of the server, defined as the probability of a non-empty queue. The server occupation is

$$\begin{aligned} U &:= P(Q > 0) \\ &= 1 - P(Q = 0) \\ &= 1 - \pi_0 \\ &= 1 - \frac{1-\rho}{1-\rho^{K+1}} \\ &= \rho\left(\frac{1-\rho^K}{1-\rho^{K+1}}\right) \qquad (3.5) \\ &= \rho\,(1 - P_L). \qquad (3.6) \end{aligned}$$

Again, we can derive from the expression for U the following expression for K in terms of ρ and U,

$$K = \frac{1}{\log \rho} \cdot \log\left(\frac{1 - U/\rho}{1 - U}\right). \qquad (3.7)$$

3.4 The expected response time

The expected response time is an interesting metric and of relative importance depending on the application and its needs. To express this quantity, we first define T_n as the response time of the n-th foreground packet. It follows that $T_n = d_n - a_n$. Again, let $T = \lim_{n\to\infty} T_n$ then, the expected response time is

$$\begin{aligned} R &= E[\,T \mid X = 0\,] \\ &= \frac{\sum_{i=0}^{K-1} (i+1)\,\pi(i)}{\mu(1 - \pi_K)} \qquad (3.8) \end{aligned}$$

since a customer waits for $(i+1)/\mu$ units of time if there were already i customers in the queue; $1 - \pi_K$ is the probability of a success. Using (3.2) we can write

$$R = \frac{1}{\mu\,(1-\pi_K)}\left(\frac{1-\rho}{1-\rho^{K+1}} \sum_{i=0}^{K-1} (i+1)\,\rho^i\right).$$

Note that $\sum_{i=0}^{K-1} (i+1)\,\rho^i$ is the derivative of $\sum_{i=0}^{K-1} \rho^{i+1} = \rho\,\frac{1-\rho^K}{1-\rho}$ with respect to the variable ρ. Hence,

$$\begin{aligned} R &= \frac{1}{\mu\,(1-\pi_K)}\left(\frac{1-\rho^K}{(1-\rho)\,(1-\rho^{K+1})} - K\,\frac{\rho_K}{1-\rho^{K+1}}\right) \qquad (3.9) \\ &= \frac{1}{\mu\,(1-\rho)} - \frac{K}{\mu}\,\frac{\pi_K}{(1-\rho)\,(1-\pi_K)}. \qquad (3.10) \end{aligned}$$

In other words, R is the expected response time of non-lost foreground customers. The last expression for R, which was derived from (3.9) and (3.2), will prove useful. We can express R only in terms of ρ and K by replacing π_K given by (3.3) in (3.10). This gives

$$R = \frac{1}{\mu(1-\rho)} - \frac{K}{\mu}\frac{\rho^K}{1-\rho^K}. \tag{3.11}$$

Observe that the expected response time of non-lost foreground customers is larger than or equal to their expected service time, namely,

$$R \geq \frac{1}{\mu}. \tag{3.12}$$

3.5 The conditional loss probability

The next metric we are going to study is the conditional loss probability, or in other words, the probability that two successive losses occur. To be able to express this conditional probability, we define $p_{i,j} = P(Q_n = j \mid Q_{n-1} = i)$, $0 \leq i, j \leq K$. The following equations describe the behavior of these probabilities:

$$\begin{aligned} p_{i,j} &= \frac{\mathbf{1}\{j=i+1\}\gamma + \lambda p_{i+1,j} + \mu p_{i-1,j}}{\gamma+\lambda+\mu} && 0 < i < K,\ 0 \leq j \leq K \\ p_{0,j} &= \frac{\mathbf{1}\{j=1\}\gamma + \lambda p_{1,j}}{\gamma+\lambda} && 0 \leq j \leq K \\ p_{K,j} &= \frac{\mathbf{1}\{j=K\}\gamma + \mu p_{K-1,j}}{\gamma+\mu} && 0 \leq j \leq K. \end{aligned}$$

The conditional probability q_L that a foreground customer is lost given that the previous foreground customer is lost is $q_L = p_{K,K}$. q_L is in fact what we have defined as the *conditional loss probability*.

To be able to derive a closed form expression for q_L, we define $N(t)$ to be the queue length of the system with the foreground source removed ($\gamma = 0$) at time $t \geq 0$. Let $P_{i,k}(t) = P(N(t) = k \mid N(0) = i)$. We have the following differential equations:

$$\frac{d}{dt}P_{i,0}(t) = -\lambda P_{i,0}(t) + \mu P_{i,1}(t) \tag{3.13}$$

$$\frac{d}{dt}P_{i,K}(t) = -\mu P_{i,K}(t) + \lambda P_{i,K-1}(t) \tag{3.14}$$

$$\frac{d}{dt}P_{i,k}(t) = -(\lambda+\mu)P_{i,k}(t) + \lambda P_{i,k-1}(t) + \mu P_{i,k+1}(t) \quad k = 1, 2, \ldots, K-1 \tag{3.15}$$

for $i = 0, 1, \ldots, K$. Define $P_i(z,t) = \sum_{k=0}^{K} P_{i,k}(t)\, z^k$. Then,

$$\begin{aligned} z\frac{d}{dt}P_i(z,t) &= z\frac{d}{dt}\sum_{k=0}^{K} P_{i,k}(t)\, z^k \\ &= z\sum_{k=0}^{K}\frac{d}{dt}P_{i,k}(t)\, z^k \\ &= z\left(\frac{d}{dt}P_{i,0}(t) + \sum_{k=1}^{K-1}\frac{d}{dt}P_{i,k}(t)\, z^k + \frac{d}{dt}P_{i,K}(t)\, z^K\right). \end{aligned}$$

Using equations (3.13) – (3.15) and after some algebra we get

$$z\frac{d}{dt}P_i(z,t) = (1-z)\left[(\mu - \lambda z)P_i(z,t) - \mu P_{i,0}(t) + \lambda z^{K+1} P_{i,K}(t)\right]. \tag{3.16}$$

Now we consider the Laplace transform of $P_i(z,t)$, $P_i^*(z,s) = \int_0^\infty e^{-st} P_i(z,t)\, dt$. Replacement of this in (3.16) along with the use of the following relation

$$\int_0^\infty e^{-st}\frac{d}{dt}\, P_i(z,t)\, dt = sP_i^*(z,s) - P_i(z,0)$$

and some algebraic manipulations yields

$$P_i^*(z,s) = \frac{z^{i+1} - \mu(1-z)P_{i,0}^*(s) + \lambda(1-z)z^{K+1}P_{i,K}^*(s)}{sz - (1-z)(\mu - \lambda z)} \tag{3.17}$$

where $P_{i,k}^*(s) = \int_0^\infty e^{-st} P_{i,k}(t) dt,\ k = 0, 1, \ldots, K$. The denominator of the right-hand side of (3.17) contains two zeros,

$$\begin{aligned} z_1(s) &= \frac{\lambda + \mu + s - \sqrt{(\lambda+\mu+s)^2 - 4\lambda\mu}}{2\lambda} \\ z_2(s) &= \frac{\lambda + \mu + s + \sqrt{(\lambda+\mu+s)^2 - 4\lambda\mu}}{2\lambda} \end{aligned}$$

for $\Re(s) \geq 0$. As $P_i^*(z,s)$ is analytic, the zeros of the denominator must also be zeros of the numerator. More precisely, the numerator must satisfy

$$z_k^{i+1}(s) - (1 - z_k(s))[\mu P_{i,0}^*(s) - \lambda z_k(s)^{K+1} P_{i,K}^*(s)] = 0, \qquad k = 1, 2.$$

These two equations can be solved to yield

$$\begin{aligned} P_{i,0}^*(s) &= \frac{z_2(s)^{i+1} z_1(s)^{K+1}(1 - z_2(s))^{-1} - z_1(s)^{i+1} z_2(s)^{K+1}(1 - z_1(s))^{-1}}{\mu(z_1(s)^{K+1} - z_2(s)^{K+1})} \\ P_{i,K}^*(s) &= \frac{z_2(s)^{i+1}(1 - z_2(s))^{-1} - z_1(s)^{i+1}(1 - z_1(s))^{-1}}{\lambda(z_1(s)^{K+1} - z_2(s)^{K+1})}. \end{aligned}$$

Now, q_L is

$$\begin{aligned} q_L &= P(Q_n = K|Q_{n-1} = K) \\ &= \gamma \int_0^\infty e^{-\gamma t} P_{K,K}(t)\, dt \\ &= \gamma P^*_{K,K}(\gamma) \\ &= \gamma \frac{(1 - z_2(\gamma))^{-1} - [z_1(\gamma)/z_2(\gamma)]^{K+1}(1 - z_1(\gamma))^{-1}}{\lambda([z_1(\gamma)/z_2(\gamma)]^{K+1} - 1)}. \end{aligned} \tag{3.18}$$

Expression (3.18) for q_L can be inverted to obtain

$$K = \frac{\log(\gamma(1 - z_2(\gamma))^{-1} + q_L\lambda) - \log(\gamma(1 - z_1(\gamma))^{-1} + q_L\lambda)}{\log z_1(\gamma) - \log z_2(\gamma)} - 1. \tag{3.19}$$

3.6 The conditional non-loss probability

Another metric can also be calculated. It is the conditional probability that a foreground packet arrives to find room in the buffer given that the previous foreground customer was also admitted. We shall refer to this probability as the *conditional non-loss probability* and it will be denoted by q_N. We have

$$\begin{aligned} q_N &= P(Q_{n+1} \neq K \,|\, Q_n \neq K) \\ &= \sum_{i=0}^{K-1} \frac{P(Q_{n+1} \neq K, Q_n = i, Q_n \neq K)}{P(Q_n \neq K)} \\ &= \sum_{i=0}^{K-1} \frac{P(Q_{n+1} \neq K \,|\, Q_n = i)\, \pi(i)}{1 - \pi(K)} \\ &= \sum_{i=0}^{K-1} \frac{(1 - P(Q_{n+1} = K \,|\, Q_n = i))\, \pi(i)}{1 - \pi(K)}. \end{aligned}$$

Recall the definition of $P_{i,k}(t) = P(N(t) = k \,|\, N(0) = i)$, where $N(t)$ is the queue-length at time t when $\gamma = 0$ (no foreground customers). Since the n-th foreground customer is accepted in the system when $Q_n = i < K$, we have

$$\begin{aligned} P(Q_{n+1} = K \,|\, Q_n = i) &= \int_0^\infty P_{i+1,K}(t)\, \gamma\, e^{-t\gamma}\, dt \\ &= \gamma\, P^*_{i+1,K}(\gamma) \end{aligned}$$

for $i = 0, 1, \ldots, K-1$, with $P^*_{j,k}(s) = \int_0^\infty e^{-st}\, P_{j,k}(t)\, dt$.

Therefore,

$$q_N = 1 - \gamma \sum_{i=1}^{K-1} \frac{P^*_{i+1,K}(\gamma)\, \pi(i)}{1 - \pi(K)}.$$

Recall the formula obtained for $P^*_{j,K}(\gamma)$. With $a = z_2(\gamma)$ and $b = z_1(\gamma)$, it reads

$$P^*_{j,K}(\gamma) = \frac{a^{j+1}/(1-a) - b^{j+1}/(1-b)}{\lambda\,(b^{K+1} - a^{K+1})}$$

for $j = 0, 1, \ldots, K$. Finally,

$$\begin{aligned} q_N &= 1 - \left(\frac{\gamma}{\lambda}\right) \left(\frac{1-\rho}{1-\rho^K}\right) \left(\frac{1}{b^{K+1} - a^{K+1}}\right) \\ &\times \left[\left(\frac{a^2}{1-a}\right)\left(\frac{1-(\rho a)^K}{1-\rho a}\right) - \left(\frac{b^2}{1-b}\right)\left(\frac{1-(\rho b)^K}{1-\rho b}\right)\right]. \end{aligned} \tag{3.20}$$

Chapter 4

The M+M/D/1/K queue

4.1 The model

We still consider the model introduced in Section 3.1 but we now relax the assumption that the service times are exponentionally distributed. Instead we will assume that the service times are constant and equal to $1/\mu$. In the previous chapter, we explained our choice for exponentially distributed service times by the fact that various packet lengths are possible. Taking into consideration that packet lengths may not be so variable to justify the choice of an exponential distribution, we study here the extreme case: the service times are taken to be constant (i.e. all packets have the same length) with value $\sigma = 1/\mu$. Recall the definition of the traffic intensity

$$\rho \quad = \quad \frac{\lambda + \gamma}{\mu}. \tag{4.1}$$

Again, let $\{Q_n\}_{n=1}^{\infty}$ be the process of the number of packets in the queue at time of the n-th arrival from foreground source and let $Q = \lim_{n\to\infty} Q_n$. Some preliminary results must be introduced before the computation of the stationary distribution of Q.

Let $\mathcal{F}(\theta) = \mathbf{E}[\exp(-\theta\sigma)]$ $(\Re(\theta) \geq 0)$ be the Laplace-Stieltjes transform (LST) of the service time distribution. Since we consider a constant service time, this transform rewrites as $\mathcal{F}(\theta) = \exp(-\theta\sigma)$. For $\rho \geq 0$ and $|z| \leq 1$, define

$$\begin{aligned} \mathcal{G}_\rho(z) &= \mathcal{F}\left(\frac{\rho\,(1-z)}{\bar{\sigma}}\right) - z \\ &= \exp\left(-\frac{\sigma\,\rho\,(1-z)}{\bar{\sigma}}\right) - z \\ &= e^{-\rho\,(1-z)} - z. \end{aligned} \tag{4.2}$$

For $\rho \geq 0$, we denote by $z_0(\rho)$ the zero of $\mathcal{G}_\rho(z)$ having the smallest modulus.

To express the stationary distribution of Q, we base our calculus on Cohen's analysis of the M/G/1 queue with finite waiting room [5, Chapter III.6]. Introduce the parameter B defined as

$$B = 1 + \frac{\rho}{2\pi i} \oint_{D_r} \frac{1}{\mathcal{G}_\rho(z)} \cdot \frac{dz}{z^{K-1}} \tag{4.3}$$

with D_r any circle in the complex plane with center 0 and radius strictly less than $z_0(\rho)$[1]. According to the results obtained by Cohen [5, page 575], we have

$$P(Q=0) = \frac{1}{B} \tag{4.4}$$

$$P(Q=j) = \frac{1}{2\pi i B} \oint_{D_r} \frac{1-e^{-\rho(1-z)}}{e^{-\rho(1-z)}-z} \cdot \frac{dz}{z^j}, \quad j=1,\ldots,K-1$$

$$P(Q=K) = \frac{1}{2\pi i B} \oint_{D_r} \frac{1}{e^{-\rho(1-z)}-z} \cdot \left(\rho - \frac{1-e^{-\rho(1-z)}}{1-z}\right) \cdot \frac{dz}{z^{K-1}}.$$

Using expression (4.2), the last two expressions rewrite as

$$P(Q=j) = \frac{1}{2\pi i B} \oint_{D_r} \left(\frac{1-z}{\mathcal{G}_\rho(z)} - 1\right) \cdot \frac{dz}{z^j}, \quad j=1,\ldots,K-1 \tag{4.5}$$

$$P(Q=K) = \frac{1}{2\pi i B} \oint_{D_r} \left(\frac{\rho-1}{\mathcal{G}_\rho(z)} + \frac{1}{1-z}\right) \cdot \frac{dz}{z^{K-1}}. \tag{4.6}$$

The integrals in the right-hand sides of (4.5) and (4.6) can be evaluated by the theorem of residues [17]. More precisely, the formula which is to be used is

$$\oint_C f(z)dz = 2\pi i \sum_{k=1}^{n} Res[f, z_k] \tag{4.7}$$

where $(z_1, \ldots, z_n)$ are the poles of the meromorphic function[2] f inside the circle C. To calulate a residue, use the identity

$$Res[f, z_k] = \frac{1}{(j-1)!} \left(\frac{d^{(j-1)}}{dz^{j-1}} (z-z_k)^j f(z)\right)_{z=z_k} \tag{4.8}$$

[1] a point z in the complex plane is considered to be smaller than another point z' if $|z| < |z'|$.

[2] A meromorphic function is a rational function, i.e. it has no essential singular points; for instance $f(z) = e^{(1/z)}$ is not a meromorphic function since 0 is a singular essential point.

where j is the multiplicity of pole z_k.

It must now be clear that

$$\frac{1}{2\pi i}\oint_{D_r}\frac{1}{1-z}\cdot\frac{dz}{z^{K-1}} \;=\; 1$$

and

$$\frac{1}{2\pi i}\oint_{D_r}\frac{dz}{z^j} \;=\; \mathbf{1}\{j=1\}.$$

Hence, (4.5) and (4.6) rewrite as

$$P(Q=j) \;=\; \frac{1}{B}\left[\frac{1}{2\pi i}\oint_{D_r}\frac{1}{\mathcal{G}_\rho(z)}\cdot\frac{dz}{z^j}-\frac{1}{2\pi i}\oint_{D_r}\frac{1}{\mathcal{G}_\rho(z)}\cdot\frac{dz}{z^{j-1}}-\mathbf{1}\{j=1\}\right] \tag{4.9}$$

$$P(Q=K) \;=\; \frac{1}{B}\left[\frac{\rho-1}{2\pi i}\oint_{D_r}\frac{1}{\mathcal{G}_\rho(z)}\cdot\frac{dz}{z^{K-1}}+1\right]. \tag{4.10}$$

Using (4.7) and (4.8), we find

$$\frac{1}{2\pi i}\oint_{D_r}\frac{1}{\mathcal{G}_\rho(z)}\cdot\frac{dz}{z^{j-1}} = \begin{cases} 0 & \text{if } j=1 \\ Res\left[\frac{1}{\mathcal{G}_\rho(z)}\cdot\frac{1}{z^{j-1}},0\right] & \text{if } j=2,3,\ldots \end{cases}$$

$$Res\left[\frac{1}{\mathcal{G}_\rho(z)}\cdot\frac{1}{z^{j-1}},0\right] \;=\; \frac{1}{(j-2)!}\left(\frac{d^{(j-2)}}{dz^{j-2}}\frac{1}{\mathcal{G}_\rho(z)}\right)_{z=0} \;=\; \alpha_j(\rho) \tag{4.11}$$

where $\alpha_j(\rho) = [z^{j-2}]\frac{1}{\mathcal{G}_\rho(z)}$. We denote by $[z^n]f$ the coefficient of z^n in the Taylor series expansion of f. Finally, from (4.3), (4.4), (4.9), (4.10) and (4.11), the distribution of Q is given by

$$\pi_0 \;=\; P(Q=0) \;=\; \frac{1}{1+\rho\,\alpha_K(\rho)} \tag{4.12}$$

$$\pi_1 \;=\; P(Q=1) \;=\; \frac{\alpha_2(\rho)-1}{1+\rho\,\alpha_K(\rho)} \tag{4.13}$$

$$\pi_j \;=\; P(Q=j) \;=\; \frac{\alpha_{j+1}(\rho)-\alpha_j(\rho)}{1+\rho\,\alpha_K(\rho)}, \qquad j=2,\ldots,K-1 \tag{4.14}$$

$$\pi_K \;=\; P(Q=K) \;=\; \frac{1+(\rho-1)\,\alpha_K(\rho)}{1+\rho\,\alpha_K(\rho)}. \tag{4.15}$$

π_j is the probability of having j customers in the queue.

4.2 The loss probability

Recall the definition of X_n introduced in the previous chapter, $X_n = \mathbf{1}\{Q_n = K\}$ and $X = \lim_{n\to\infty} X_n$. A customer n is lost whenever $X_n = 1$ and is not lost otherwise.

The probability that a foreground customer is lost, is the probability that it finds the system full, namely,

$$\begin{aligned} P_L &:= P(X = 1) \\ &= P(Q = K) \\ &= \pi_K = \frac{1 + (\rho - 1)\,\alpha_K(\rho)}{1 + \rho\,\alpha_K(\rho)}. \end{aligned} \tag{4.16}$$

4.3 The server occupation

The occupation U of the server was defined as the probability of a non-empty queue. The server occupation is

$$\begin{aligned} U &:= P(Q > 0) \\ &= 1 - P(Q = 0) \\ &= 1 - \frac{1}{1 + \rho\,\alpha_K(\rho)} \\ &= \frac{\rho\,\alpha_K(\rho)}{1 + \rho\,\alpha_K(\rho)} \end{aligned} \tag{4.17}$$

4.4 The expected response time

Recall the expression for the expected response time of non-lost customers in M+M/M/1/K queue (3.8)

$$R = \frac{\sum_{j=0}^{K-1} (j+1)\,\pi(j)}{\mu(1 - \pi_K)}.$$

This expression provides an upper bound for the expected response time in a M+M/D/1/K queueing system, since the expected residual time in that queue is clearly less than the expected service time (while in the M+M/M/1/K queue both quantities are equal, thanks to the memoryless property of the exponential distribution).

In the following we will use this upper bound as an approximation for R. It is however worth pointing out that an exact (but involved) formula can be derived for R in the case of the M+M/D/1/K queue (see [5, Chapter III.6, page 577]). Using equations (4.12), (4.13), (4.14) and (4.15), we can write

$$R = \frac{K\,\alpha_K(\rho) - 1 - \sum_{j=2}^{K-1} \alpha_j(\rho)}{\mu\,\alpha_K(\rho)} \tag{4.18}$$

Recall that $\alpha_j(\rho) = \frac{1}{(j-2)!} \left(\frac{d^{(j-2)}}{dz^{j-2}} \frac{1}{\mathcal{G}_\rho(z)} \right)_{z=0}, \qquad j = 2, 3, \ldots, K.$

Again, note that the expected response time of non lost foreground customers is larger than or equal to the expected service time, namely,

$$R \geq \frac{1}{\mu}. \tag{4.19}$$

From (4.18) and (4.19), we obtain the following condition

$$\begin{aligned} K\,\alpha_K(\rho) - 1 - \sum_{j=2}^{K-1} \alpha_j(\rho) &\geq \alpha_K(\rho) \\ \alpha_K(\rho) &\geq \frac{1 + \sum_{j=2}^{K-1} \alpha_j(\rho)}{K-1}. \end{aligned} \tag{4.20}$$

Chapter 5

Using the inference model

5.1 An inference question

Till now, we have introduced two models for a connection. In the first model we were able to identify five parameters describing the quality of service provided to the foreground source, namely, (3.3), (3.5), (3.11), (3.18) and (3.20),

$$
\begin{aligned}
P_L &= \frac{(1-\rho)\,\rho^K}{1-\rho^{K+1}} \\
U &= \rho\left(\frac{1-\rho^K}{1-\rho^{K+1}}\right) \\
R &= \frac{1}{\mu\,(1-\rho)} - \frac{K}{\mu}\,\frac{\rho^K}{1-\rho^K} \\
q_L &= \left(\frac{\gamma}{\lambda}\right)\left(\frac{(1-a)^{-1}-[b/a]^{K+1}(1-b)^{-1}}{[b/a]^{K+1}-1}\right) \\
q_N &= 1-\left(\frac{\gamma}{\lambda}\right)\left(\frac{1-\rho}{1-\rho^K}\right)\left(\frac{1}{b^{K+1}-a^{K+1}}\right) \\
&\times \left[\left(\frac{a^2}{1-a}\right)\left(\frac{1-(\rho a)^K}{1-\rho a}\right)-\left(\frac{b^2}{1-b}\right)\left(\frac{1-(\rho b)^K}{1-\rho b}\right)\right]
\end{aligned}
$$

where

$$
\begin{aligned}
a \;=\; z_2(\gamma) &= \frac{\lambda+\mu+\gamma+\sqrt{(\lambda+\mu+\gamma)^2-4\lambda\mu}}{2\lambda} \\
b \;=\; z_1(\gamma) &= \frac{\lambda+\mu+\gamma-\sqrt{(\lambda+\mu+\gamma)^2-4\lambda\mu}}{2\lambda}.
\end{aligned}
$$

Since $\rho = \dfrac{\lambda+\gamma}{\mu}$, all these equations are expressed in terms of λ, μ and K.

In the second model we were only able to identify three parameters, namely, (4.16), (4.17) and (4.18),

$$P_L = \frac{1 + (\rho - 1)\,\alpha_K(\rho)}{1 + \rho\,\alpha_K(\rho)}$$

$$U = \frac{\rho\,\alpha_K(\rho)}{1 + \rho\,\alpha_K(\rho)}$$

$$R = \frac{K\,\alpha_K(\rho) - 1 - \sum_{j=2}^{K-1} \alpha_j(\rho)}{\mu\,\alpha_K(\rho)}$$

where $\alpha_j(\rho) = \frac{1}{(j-2)!}\left(\frac{d^{(j-2)}}{dz^{j-2}}\frac{1}{\mathcal{G}_\rho(z)}\right)_{z=0} = [z^{j-2}]\frac{1}{\mathcal{G}_\rho(z)},\ j = 2, 3, \ldots, K.$

Since a closed-form expression for $\alpha_j(\rho)$ is not available, the only way to have an expression for it is to use a *symbolic computation software*, such as Maple V, that can give $[z^{j-2}]\frac{1}{\mathcal{G}_\rho(z)}$ for a fixed j. Looking at expression (4.18), we see that there are $K+2$ unknown quantities including R. For this reason, expression for R cannot be used to estimate λ and K. In fact, only equations (4.16) and (4.17) are useful at the moment.

Our purpose is to use these models to infer the *buffer size* and the *intensity of cross traffic* at the bottleneck link of a path between two hosts. The bandwidth of the bottleneck is supposed to be known, since various methods are available to estimate it [1, 4, 12]. The problem is therefore the following: How can we infer estimates $\hat{\lambda}_n$ and $\hat{K}_n$ from the observations collected by the first n probe packets?

Only two equations in terms of λ and K are necessary for this. In other words, $\hat{\lambda}_n$ and $\hat{K}_n$ can be inferred from two equations to be chosen among (3.3), (3.5), (3.11), (3.18) and (3.20) for the M+M/M/1/K. This gives rise to ten possible schemes for estimating λ and K, namely,

1. Estimate P_L and U and use equations (3.3) and (3.5) to determine $\hat{\rho}_n$ and $\hat{K}_n$ (hereafter referred to as scheme **I**).

2. Estimate P_L and R and use equations (3.3) and (3.11) to determine $\hat{\rho}_n$ and $\hat{K}_n$ (hereafter referred to as scheme **II**).

3. Estimate P_L and q_L and use equations (3.3) and (3.18) to determine $\hat{\rho}_n$ and $\hat{K}_n$ (hereafter referred to as scheme **III**).

4. Estimate P_L and q_N and use equations (3.3) and (3.20) to determine $\hat{\rho}_n$ and $\hat{K}_n$ (hereafter referred to as scheme **IV**).

5. Estimate U and R and use equations (3.5) and (3.11) to determine $\hat{\rho}_n$ and $\hat{K}_n$ (hereafter referred to as scheme **V**).

6. Estimate U and q_L and use equations (3.5) and (3.18) to determine $\hat{\rho}_n$ and $\hat{K}_n$ (hereafter referred to as scheme **VI**).
7. Estimate U and q_N and use equations (3.5) and (3.20) to determine $\hat{\rho}_n$ and $\hat{K}_n$ (hereafter referred to as scheme **VII**).
8. Estimate R and q_L and use equations (3.11) and (3.18) to determine $\hat{\rho}_n$ and $\hat{K}_n$ (hereafter referred to as scheme **VIII**).
9. Estimate R and q_N and use equations (3.11) and (3.20) to determine $\hat{\rho}_n$ and $\hat{K}_n$ (hereafter referred to as scheme **IX**).
10. Estimate q_L and q_N and use equations (3.18) and (3.20) to determine $\hat{\rho}_n$ and $\hat{K}_n$ (hereafter referred to as scheme **X**).

For the M+M/D/1/K model, only two equations are available. Estimating P_L and U and using (4.16) and (4.17) will provide $\hat{\rho}_n$ and $\hat{K}_n$ (hereafter referred to as scheme **XI**).

In total, eleven schemes are available. Based on simulations and analysis, we will try to identify the best one for criterias such as: fast convergence, small latency added at the source, minimum variance, existence and uniqueness of the solution, biased or unbiased estimators, etc.

5.2 Solving for the equations

Analytical solution for each scheme is hard to find since some expressions like (3.11) and (3.20) cannot easily be inverted. However, it is possible to prove the existence and the uniqueness of the solutions except for scheme **IX** as none of the equations giving R and q_N could be inverted. We will discuss here only a few schemes.

5.2.1 Solving for scheme I

The two equations considered here are (3.3) and (3.5)

$$\begin{aligned} P_L &= \frac{(1-\rho)\,\rho^K}{1-\rho^{K+1}} \\ U &= \rho\left(\frac{1-\rho^K}{1-\rho^{K+1}}\right) \\ &= \rho\,(1-P_L). \end{aligned}$$

It follows

$$\rho = \frac{U}{1-P_L}.$$

Using (3.7), we find

$$K = \frac{\log(P_L/(1-U))}{\log(U/(1-P_L))}.$$

To obtain λ, use the relation

$$\lambda = \frac{\mu U}{1-P_L} - \gamma.$$

Observe that whenever $U = 1$ and $P_L \neq 1$, K cannot be computed with this scheme. In this case the solution returned is $K = \infty$.

5.2.2 Solving for scheme XI

This scheme still involves P_L and U, but this time for the M+M/D/1/K model. The equations are (4.16) and (4.17)

$$\begin{aligned} P_L &= \frac{1 + (\rho - 1)\,\alpha_K(\rho)}{1 + \rho\,\alpha_K(\rho)} \\ U &= \frac{\rho\,\alpha_K(\rho)}{1 + \rho\,\alpha_K(\rho)}. \end{aligned}$$

As already mentioned, no analytical expression for $\alpha_K(\rho)$ is available. To obtain K and λ, we therefore proceed as follows. First, we compute

$$\rho = \frac{U}{1-P_L}$$

and

$$\alpha_K(\rho) = \frac{1-P_L}{1-U}. \tag{5.1}$$

Since a numeric value for ρ is available, we use a *symbolic computation software*, such as Maple V to compute the coefficients $[z^{j-2}]\frac{1}{\mathcal{G}_\rho(z)}$ for a certain range of j and compare them with the value obtained for $\alpha_K(\rho)$. The closest match obtained for j^* will provide $K = j^*$. As before, to obtain λ, use the relation

$$\lambda = \frac{\mu U}{1-P_L} - \gamma.$$

When $U = 1$ while $P_L \neq 1$, (5.1) returns $\alpha_K(\rho) = \infty$. No match is found with any of the coefficients in the Taylor series expansion of $\frac{1}{\mathcal{G}_\rho(z)}$ and K is undefined. Notice that ρ_I[1] and ρ_{XI} have the same expression, hence both schemes **I** and **XI** return the same estimated value for λ.

[1]We mean by this notation "ρ provided by scheme **I**"

5.2.3 Existence and uniqueness of the solution of scheme V

Scheme **V** involves equations (3.5) and (3.11)

$$\begin{aligned} U &= \rho \left(\frac{1-\rho^K}{1-\rho^{K+1}} \right) \\ R &= \frac{1}{\mu(1-\rho)} - \frac{K}{\mu} \frac{\rho^K}{1-\rho^K}. \end{aligned} \tag{5.2}$$

Another expression (3.10) for R was found to be useful here

$$R = \frac{1}{\mu(1-\rho)} - \frac{K}{\mu} \frac{\pi_K}{(1-\rho)(1-\pi_K)}, \tag{5.3}$$

which is obtained from (5.2) by using (3.2). Using (3.6), π_K can be expressed as

$$\pi_K = 1 - U/\rho, \tag{5.4}$$

to yield from (5.3)

$$R = \frac{1}{\mu(1-\rho)} - \frac{K}{\mu} \frac{\rho - U}{(1-\rho)U}. \tag{5.5}$$

Recall the relation (3.7) for K

$$K = \frac{1}{\log \rho} \cdot \log \left(\frac{1-U/\rho}{1-U} \right).$$

Plugging equation (3.7) for K into (5.5) gives

$$R = \frac{1}{\mu(1-\rho)} - \frac{\rho - U}{\mu U(1-\rho) \log \rho} \log . \left(\frac{\rho - U}{\rho(1-U)} \right). \tag{5.6}$$

Observe that necessarily $\rho \geq U$. For $\rho \geq U$, introduce the mapping

$$f(x) = \frac{1}{\mu(1-x)} - \frac{x-U}{\mu U(1-x) \log x} \log \left(\frac{x-U}{x(1-U)} \right) - R. \tag{5.7}$$

If one can show that the equation $f(x) = 0$ has a unique solution in $[U, \infty)$, then this solution will give us ρ, and subsequently K by using (3.7). Proposition 5.2.1 shows that this is indeed the case.

Proposition 5.2.1 *For any constants $\mu > 0$, $0 \leq U \leq 1$ and $R \geq 1/\mu$, the equation $f(x) = 0$ has a unique solution in $[U, \infty)$.*

Proof.
Define

$$g(x) = U \log x - (x-U) \log \left(\frac{x-U}{x(1-U)} \right) - \mu R U (1-x) \log x$$

for $x \geq U$. Hence (5.7) rewrites as

$$f(x) = \frac{g(x)}{\mu U (1-x) \log x}. \tag{5.8}$$

Denote by $g^{(1)}(x)$ (resp. $g^{(2)}(x)$) the first (resp. second) order derivative of $g(x)$. We find

$$g^{(1)}(x) = \mu RU \log x - \mu RU \frac{1-x}{x} - \log\left(\frac{x-U}{x(1-U)}\right) \tag{5.9}$$

and

$$\begin{aligned} g^{(2)}(x) &= \frac{\mu RU}{x} + \frac{\mu RU}{x^2} - \frac{U}{x(x-U)} \\ &= \frac{U\,h(x)}{x^2 (x-U)} \end{aligned} \tag{5.10}$$

with

$$\begin{aligned} h(x) &= \mu Rx(x-U) + \mu R(x-U) - x \\ &= \mu R(x-U)(x+1) - x \\ &= \mu Rx^2 - [1-\mu R(1-U)]\,x - \mu RU. \end{aligned} \tag{5.11}$$

The function $h(x)$ has two zeros

$$\begin{aligned} x_1 &= \frac{1-\mu R(1-U) - \sqrt{[1-\mu R(1-U)]^2 + 4\mu^2 R^2 U}}{2\mu R} \\ x_2 &= \frac{1-\mu R(1-U) + \sqrt{[1-\mu R(1-U)]^2 + 4\mu^2 R^2 U}}{2\mu R}. \end{aligned}$$

It is clear that $x_1 \leq 0$. As for x_2, notice that $h(U) = -U \leq 0$. Since $h(x_2) = 0$ and $\lim_{x\to\pm\infty} h(x) = +\infty$, it follows that $x_2 \geq U$. Hence the function $h(x)$ has only one zero in $[U, \infty)$.

Looking at expression (5.8), we can say that the zeros of $g(x)$ are the zeros of $f(x)$; however, the value $x = 1$ is a particular case. We have $g(1) = 0$, $g^{(1)}(1) = 0$ and $g^{(2)}(1) = 2\mu RU - U/(1-U)$. By applying l'Hôpital's rule to the right-hand side of (5.8), we see that $f(1)$ is well-defined, with value

$$\begin{aligned} f(1) &= \frac{g^{(2)}(1)}{-2\mu U} \\ &= \frac{1-2\mu R(1-U)}{2\mu(1-U)}. \end{aligned} \tag{5.12}$$

$f(1) = 0$ if and only if $g^{(2)}(1) = 0$ i.e. if $1 - 2\mu R(1-U) = 0$. Therefore, unless this condition is satisfied, the zeros of $f(x)$ in $[U, \infty)$ are the zeros of

$g(x)$ in $[U, \infty) - \{1\}$; for $1 - 2\mu R\,(1 - U) = 0$, the zeros of $f(x)$ in $[U, \infty)$ are the zeros of $g(x)$ in $[U, \infty)$. In that case, (5.11) rewrites as

$$h(x) \;=\; \frac{1}{2\,(1-U)}\,(x^2 - x(1-U) - U)$$

and $x_1 = 1$ and $x_2 = -U$. Three cases are to be studied depending on whether x_1 is less, equal or greater than 1. In each case the variations of the functions $g(x)$ and $f(x)$ are studied. We aim to show that $g(x)$ has a unique zero in $[U, \infty) - \{1\}$ when $g^{(2)}(1) \neq 0$ and a unique zero in $[U, \infty)$, located at the point $x = 1$, when $g^{(2)}(1) = 0$, which will conclude the proof. The following limits are easily calculated

$$\begin{aligned}
\lim_{x \to +\infty} g^{(2)}(x) &= 0 \\
\lim_{x \to -\infty} g^{(2)}(x) &= -\infty \\
\lim_{x \to \pm\infty} g^{(1)}(x) &= +\infty \\
\lim_{x \to +\infty} g(x) &= +\infty.
\end{aligned}$$

- $U \leq x_1 \leq 1$

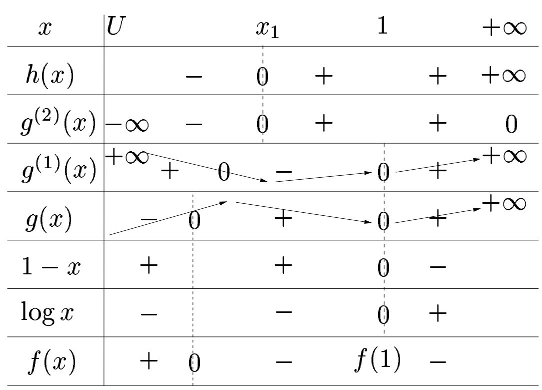

Figure 5.1: $U \leq x_1 \leq 1$

We conclude from Figure 5.1 that $g(x)$ has a unique zero in $[U, \infty) - \{1\}$ when $U \leq x_1 \leq 1$. This zero is located in $[U, x_1)$

- $x_1 \geq 1$

x	U		1		x_1				$+\infty$
$h(x)$			$-$		0		$+$		$+\infty$
$g^{(2)}(x)$	$-\infty$		$-$		0		$+$		0
$g^{(1)}(x)$	$+\infty$	$+$ ↘	0	$-$ ↘		0		$+$ ↗	$+\infty$
$g(x)$		$-$ ↗	0	$-$ ↘			0	$+$ ↗	$+\infty$
$1-x$		$+$	0	$-$				$-$	
$\log x$		$-$	0	$+$				$+$	
$f(x)$		$+$	$f(1)$	$+$			0	$-$	

Figure 5.2: $x_1 \geq 1$

We conclude from Figure 5.2 that $g(x)$ has a unique zero in $[U, \infty) - \{1\}$ when $x_1 \geq 1$. This zero is located in (x_1, ∞)

- $x_1 = 1$ (i.e. $1 - 2\mu R(1 - U) = 0$)

x	U		$x_1 = 1$		$+\infty$
$h(x)$		$-$	0	$+$	$+\infty$
$g^{(2)}(x)$	$-\infty$	$-$	0	$+$	0
$g^{(1)}(x)$	$+\infty$	$+$ ↘	0	$+$ ↗	$+\infty$
$g(x)$		$-$ ↗	0	$+$ ↗	$+\infty$
$1-x$		$+$	0	$-$	
$\log x$		$-$	0	$+$	
$f(x)$		$+$	0	$-$	

Figure 5.3: $x_1 = 1$

In this case (cf. Figure 5.3), $g(x)$ has only one zero in $[U, \infty)$ which is $x_1 = 1$.

5.2.4 About the other schemes

As for the eight schemes left, existence and uniqueness of the solution of only scheme **II** has been proved by P. Nain and D. Towsley. Proofs for schemes **III**, **IV** and **VI** through **X** are still to be done.

Schemes **II** through **X** were solved for numerically with Maple V. To do so Maple uses a variation on Newton's method, thus producing approximate solutions.

5.3 Calculating the moment-based estimators

We have at our disposal the first n samples of $\{X_i\}$, $\{a_i\}$, $\{d_i\}$, and we know γ and μ. Let $\hat{U}(n)$, $\hat{P}_L(n)$, $\hat{R}(n)$, $\hat{q}_L(n)$ and $\hat{q}_N(n)$ denote the estimators of U, P_L, R, q_L and q_N, respectively. They are defined as $(n = 1, 2, \ldots)$

$$\hat{P}_L(n) := \frac{1}{n}\sum_{i=1}^{n} X_i \tag{5.13}$$

$$\hat{U}(n) := \frac{1}{n}\sum_{i=1}^{n} \mathbf{1}(\sigma_i \neq d_i - a_i) \tag{5.14}$$

$$\hat{R}(n) := \frac{\sum_{i=1}^{n}(1-X_i)\,(d_i - a_i)}{\sum_{i=1}^{n}(1-X_i)}, \qquad \text{for } \sum_{i=1}^{n}(1-X_i) > 0 \tag{5.15}$$

$$\hat{q}_L(n) := \frac{\sum_{i=1}^{n-1} X_i X_{i+1}}{\sum_{i=1}^{n-1} X_i}, \qquad \text{for } \sum_{i=1}^{n-1} X_i > 0 \tag{5.16}$$

$$\hat{q}_N(n) := \frac{\sum_{i=1}^{n-1}(1-X_i)(1-X_{i+1})}{n - \sum_{i=1}^{n-1} X_i}, \qquad \text{for } \sum_{i=1}^{n-1} X_i < n \tag{5.17}$$

where σ_i denotes the service time of the i-th foreground customer (assumed to be available).

5.4 Desirable properties of estimators

If a comparison is to be made among several estimators, it is useful to have in mind the main properties of a good estimator [21]. Namely:

- No bias: an unbiased estimator is one that is, *on the average*, right on target. Formally, the definition is,

  $$\hat{\theta} \text{ is an unbiased estimator of } \theta \text{ if } E(\hat{\theta}) = \theta.$$

  An estimator is called biased if $E(\hat{\theta})$ is different from θ; in fact, bias is defined as this difference,

  $$\text{Bias} \triangleq E(\hat{\theta}) - \theta.$$

  The distribution of $\hat{\theta}$ is said to be "off target".

- Efficiency: As well as being on target on the average, we also like the distribution of an estimator $\hat{\theta}$ to be highly concentrated, that is to have a small variance. This is the notion of efficiency. $\hat{\theta}$ is said to be more efficient if it has a smaller variance. Formally, the relative efficiency of two unbiased[2] estimators is defined as

$$\text{Relative efficiency of } \hat{\theta}_1 \text{ compared to } \hat{\theta}_2 \triangleq \frac{\text{var}\hat{\theta}_2}{\text{var}\hat{\theta}_1}.$$

- Consistency: Roughly speaking, a consistent estimator is one that concentrates completely on its target as the sample size increases indefinitely. In the limiting case, as the sample size becomes infinite, a consistent $\hat{\theta}$ will provide a perfect point estimate of the target θ. Formally,

  $$\hat{\theta} \text{ is consistent iff } E(\hat{\theta} - \theta)^2 \to 0 \text{ as } n \to \infty.$$

  The mean squared error is related to bias and variance by the following theorem,

  $$E(\hat{\theta} - \theta)^2 = \text{bias}(\hat{\theta})^2 + \text{var}\hat{\theta}$$

  which has the important corollary: $\hat{\theta}$ is a consistent estimator iff[3] its bias and variance *both* approach zero, as $n \to \infty$. If only the bias approaches zero, the estimator is called *asymptotically unbiased.*

[2]For biased estimators, the definition of efficiency is $\frac{E(\hat{\theta}_2-\theta)^2}{E(\hat{\theta}_1-\theta)^2}$.
[3]iff is an abbreviation for "if and only if".

Chapter 6

Simulation results and analysis

6.1 Traces generation

The series $\{a_i\}$, $\{d_i\}$, $\{X_i\}$ and $\{\sigma_i\}$ were extracted from traces generated by *ns* [11]. In total, sixteen traces were generated. For each trace, the following parameters were varied either singly or in combination with others:

- Topology of the network: three different architectures were tried, starting with a unique link between two nodes, till having three links in cascade.
- Link bandwidths and bottleneck location: in the case of more than one link, link bandwidth values were varied to have all the possible locations for the bottleneck link.
- Amount and type of cross traffic: three cases were studied, in the first one (hereafter referred to as case **A**), cross traffic was generated by a single Poisson-like source[1]. In the second case (hereafter referred to as case **B**), cross traffic was generated by an FTP application over a TCP agent. In the third case (hereafter referred to as case **C**), three flows were aggregated to give the cross traffic: two TCP flows and a CBR flow.
- Packet length: Each flow has a fixed length for its generated packets, but packets length varied from a flow to another. In case A, background and foreground traffic had packets of constant length equal to 100 bytes; in case B, probe packets length was 100 bytes and TCP packets length was 500 bytes. In case C, probes TCP and CBR packets length were 50, 450, 500 and 800 bytes respectively.

[1]The packets generated were of the same length, only interarrival times where random variables with an exponential distribution of rate λ.

- Run time: When run time is changed, the number of collected samples varies. All simulations had the same run time to collect 5000 probe packets, except for one where the number of collected probe packets was 50000.

The foreground traffic was generated by a Poisson-like source, interarrival times were i.i.d. random variables having an exponential distribution with rate $\gamma = 250ms^{-1}$; however packet lengths were not random variables as all generated packets had the same length. For each simulation, the buffer at the bottleneck had room for six customers. For case A where the background traffic was Poisson-like, the rate was taken to be $\lambda = 950ms^{-1}$. For cases B and C, the mean rate for foreground traffic was measured as the number of foreground packets arriving to the bottleneck link over the run time.

6.2 Estimating foreground traffic and buffer size

Having at our disposal $\{a_i\}$, $\{d_i\}$, $\{X_i\}$ and $\{\sigma_i\}$ for the n first packets, the moment-based estimators are calculated according to formulas (5.13), (5.14), (5.15), (5.16) and (5.17). At this point, $\hat{P}_L(n)$, $\hat{U}(n)$, $\hat{R}(n)$, $\hat{q}_L(n)$ and $\hat{q}_N(n)$ are plugged into equations (3.3), (3.5), (3.11), (3.18), (3.20), (4.16) and (4.17). The eleven couples of equations referred to as schemes **I** through **XI** are then solved numerically using Maple V to give the estimated parameters $\hat{\lambda}$ and $\hat{K}$. Results are reported in the appendix for each simulation. Schemes giving the best results for each simulation are tabulated in Table 6.1.

6.3 A first analysis of the results

Looking at the plotted results for each simulation, we observe the following:

- There are three groups of schemes giving similar results. These groups are: schemes **III - IV - X**, schemes **I - VII** and schemes **II - IX**. This fact is not surprising in the case of the first group, since the three schemes involve estimators P_L, q_L and q_N, which calculation is based on the $\{X_i\}$. It is the case when only measurements at the sender are available. As for the other two groups of schemes, scheme **I** uses U and P_L and scheme **II** uses U and q_N, scheme **II** uses R and P_L and scheme **IX** uses R and q_N. Hence, to classify the schemes within each group, we must look at the cost and latency they introduce in the application.

- Schemes **VI** and **VIII** almost never returned results. Since the existence and uniqueness of the solutions of these two schemes were not studied, we cannot provide an explanation for this at the moment.

foreground background	Case **A** Poisson (100B) Poisson (100B)	Case **B** Poisson (100B) TCP (500B)	Case **C** Poisson (50B) TCP_1 (450B) TCP_2 (500B) CBR (800B)
one link best $\hat{K}_n$ best $\hat{\lambda}_n$	**XI - III - IV - X** **XI - I - VII**	**IX - II** **XI - I - VII**	**II - IX** **XI - I - VII**
two links: 1^{st} one is the bottleneck best $\hat{K}_n$ best $\hat{\lambda}_n$	**XI - III - IV - X** **XI - I - VII**	**IX - II** **XI - I - VII**	**II - IX** **XI - I - VII**
two links: 2^{nd} one is the bottleneck best $\hat{K}_n$ best $\hat{\lambda}_n$	**XI - VII** **XI - I - VII**	Not Available Not Available	**II - IX** **IX - II**
three links: 1^{st} one is the bottleneck best $\hat{K}_n$ best $\hat{\lambda}_n$	**XI - III - IV - X** **XI - I - VII**	**IX - II** **XI - I - VII**	**IX - II** **XI - I - VII**
three links: 2^{nd} one is the bottleneck best $\hat{K}_n$ best $\hat{\lambda}_n$	**XI - III - IV - X** **XI - I - VII**	Not Available Not Available	**XI - IX - II** **IX - II**
three links: 3^{rd} one is the bottleneck best $\hat{K}_n$ best $\hat{\lambda}_n$	**XI - III - IV - X** **XI - I - VII**	Not Available Not Available	**VIII - II - IX** **IX - II**

Table 6.1: Best schemes for all simulations

- Scheme **XI** provided the best estimations for all simulation runs in case **A**, which is very normal as case **A** aproximates at best M+M/D/1/K queueing system.

- The bottleneck location has an impact on the estimated values of λ and K. Almost identical results were obtained when the bottleneck was the access to the first link. This was no longer the case when the bottleneck was the access to the second or to third link. More precisely, the estimated parameters converged much more slowly to the right values. This was expected because losses occuring elsewhere than at the bottleneck are not taken into consideration in both models studied.

- Making the run time bigger affects the number of gathered samples. We have done this for only one simulation and we noticed that the "best" scheme for a 20 seconds run time was no more the "best" one for a 200 seconds run time

Looking at Table 1, we see that the "best" scheme in estimating λ is not always the "best" scheme in estimating K. This curious fact is still to be analyzed, for no explanation is available at the moment. We can imagine an application using both schemes, each one for the estimation of just one parameter.

6.4 From simulation to reality

Till now, we have always assumed to have access to the first n samples of $\{a_i\}$, $\{d_i\}$, $\{X_i\}$ and $\{\sigma_i\}$. In this work, we have carried out simulations to generate traffic traces, and the samples were extracted from the traces. However, ultimately, we must extract the samples from the real network (e.g. the Internet). How can we do this?

Usually, real-time applications use the Real-Time Transport Protocol (RTP) [14] together with UDP and IP. RTP provides end-to-end network transport functions suitable for this kind of applications, over multicast or unicast network services. RTP consists of two parts, a data part and a control part referred to as RTCP, the Real-Time Control Protocol. The feedback information is carried in RTCP packets referred to as Receiver Reports (RR).The rate at which they are multicast is controlled so that the load created by the control information is a small fraction of that created by data traffic. The RR sent by a destination includes several informations: the highest sequence number received, the number of packets lost, the estimated packet interarrival jitter, and timestamps. At the sender, the $\{a_i\}$ are available, the $\{d_i\}$ are retrieved from the timestamps present in the RR and the $\{X_i\}$ are retrieved from the highest sequence number received at the destination, also given in the RR. As for the $\{\sigma_i\}$, they are hard to obtain, hence we can try to estimate U differently, by considering that a packet finds the bottleneck server empty if its response time is minimal.

Chapter 7

Conclusion

In this work, we have proposed two simple *a priori* models for a connection, based on a single server queue with finite waiting room, to infer the *buffer size* and the *intensity of cross traffic* at the bottleneck link of a path between two hosts. We have quantified several parameters of both models and obtained eleven pairs of *moment-based* estimators. Using traces generated by the network simulator *ns*, estimated values for both parameters have been calculated according to the characteristics of the *a priori* models.

A preliminary analysis of the results was conducted in the hope of "electing" the best pair of estimators. However, several drawbacks keep us from reaching simple conclusions. The experiments we made did not cover a wide range of possible test conditions and simulation run times were not long enough so that all available schemes could converge. The pairs of estimators we defined need to be tested on an experimental network, or even on the Internet, in order to quantify their performance under realistic network traffic conditions. Furthermore, a more thorough analysis of the estimators is still to be carried out, statistically (biased and unbiased estimators, confidence intervals, consistency, efficiency) and analytically (existence and uniqueness of the solutions). We must keep in mind the drawbacks of *ns*, mainly, buffer sizes are in packets not in bytes and packets length for a defined source is fixed.

For future works, other estimators can also be used like the jitter, the conditional probability of a loss knowing that the previous packet was successful and the conditional probability of a successful packet knowing that the previous one was lost. In case the robustness to statistical assumptions revealed to be weak, some hypotheses could be relaxed to be more general and other architectures for the model could be considered, a queue tandem for instance.

Bibliography

[1] J.-C. Bolot. End-to-end packet delay and loss behavior in the internet. In *Proc. of SIGCOMM'93*, pages 289–298, September 1993.

[2] J.-C. Bolot, S. Fosse-Parisis, and D. Towsley. Adaptive fec-based error control for Internet telephony. In *Proc. INFOCOM'99, New York, NY*, volume 3, pages 1453–1460, March 1999.

[3] R. Cáceres, N. G. Duffield, J. Horowitz, D. Towsley, and T. Bu. Multicast-based inference of network-internal characteristics: accuracy of packet loss estimation. In *Proc. INFOCOM'99, New York, NY*, volume 1, pages 371–379, March 1999.

[4] R. Carter and M. Crovella. Measuring bottleneck link speed in packet-switched networks. *Performance Evaluation*, 27&28:297–318, October 1996.

[5] J. W. Cohen. *The Single Server Queue.* North-Holland publishing company, 1982.

[6] S. Floyd and V. Jacobson. Random early detection gateways for congestion avoidance. *IEEE/ACM Trans. on Networking*, 1(4):397–413, August 1993.

[7] V. Jacobson. Congestion avoidance and control. In *Proc. of SIGCOMM'88*, pages 314–329, August 1988.

[8] S. Keshav. *Congestion control in computer networks.* PhD thesis, Univ. of California, Berkeley, September 1991.

[9] S. Keshav. A control-theoretic approach to flow control. In *Proc. of SIGCOMM'91*, pages 3–15, September 1991.

[10] L. Kleinrock. *Queueing Systems*, volume 1. Wiley, New York, 1975.

[11] S. McCanne and S. Floyd. *The LBNL/UCB network simulatorSoftware on line at http://www-nrg.ee.lbl.gov/ns/.* Lawrence Berkeley Lab., Univ. of California, Berkeley. Software on line at http://www-nrg.ee.lbl.gov/ns/.

[12] V. Paxson. *Measurements and analysis of end-to-end Internet dynamics.* PhD thesis, University of California at Berkeley, April 1997.

[13] S. Ratnasamy and S. McCanne. Inference of multicast routing trees and bottleneck bandwidths using end-to-end measurements. In *Proc. INFOCOM'99, New York, NY*, volume 1, pages 353–360, March 1999.

[14] H. Schulzrinne, S. Casner, R. Frederick, and V. Jacobson. RTP: a transport protocol for real-time applications. RFC 1889, Network Working Group, January 1996.

[15] V. Sharma and R. Mazumdar. Estimating traffic parameters in queueing systems with local information. *Performance Evaluation*, 32:217–230, 1998.

[16] M. Siler and J. Walrand. Monitoring quality of service: measurement & estimation. In *Proceedings of the 37th IEEE Conference on Decision & Control*, pages 539–544, 1998.

[17] E. C. Titchmarsh. *The Theory of Functions.* Oxford University Press, 2nd edition, 1939.

[18] R.-J. Vanderbei and J. Iannone. An EM approach to OD matrix estimation. Tech. rep., Princeton University, March 1994.

[19] Y Vardi. Network tomography: estimating source-destination traffic intensities. *J. Am. Statist. Assoc.*, 91:365–377, 1996.

[20] D. J. Wetherall. *Service introduction in an active network.* PhD thesis, Dept. Electrical Engineering and Computer Science, MIT, February 1999. available via http://www.sds.lcs.mit.edu/~djw/bio.html.

[21] T. H. Wonnacott and R. J. Wonnacott. *Introductory Statistics.* John Wiley & Sons, fifth edition, 1990.

Appendix

Recall the definitions for cases **A**, **B** and **C**:

- Case **A**:
  - foreground traffic: Poisson (100 bytes),
  - background traffic: Poisson (100 bytes)
- Case **B**:
  - foreground traffic: Poisson (100 bytes),
  - background traffic: TCP (500 bytes)
- Case **C**:
  - foreground traffic: Poisson (50 bytes),
  - background traffic:
    - TCP_1 (450 bytes)
    - TCP_2 (500 bytes)
    - CBR (800 bytes)

Exogeneous rate versus number of probe packets

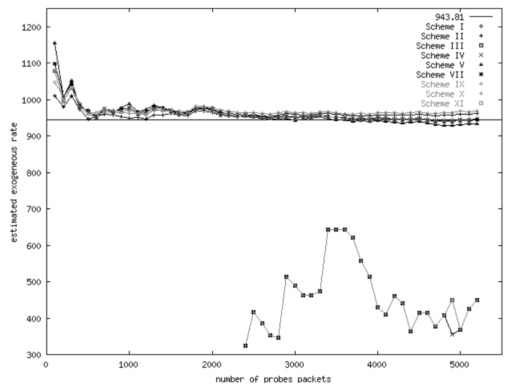

Figure 7.1: One link, case **A**

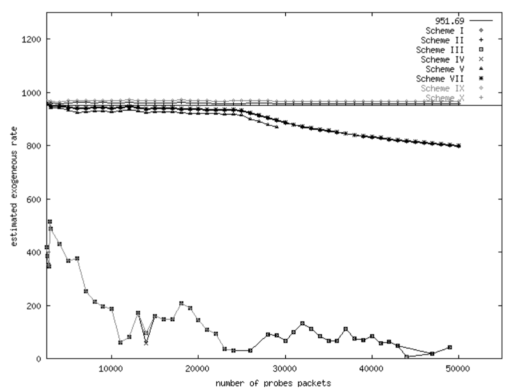

Figure 7.2: One link, case **A**, 50000 probe packets

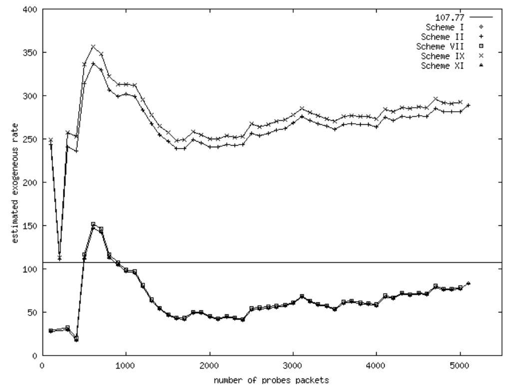

Figure 7.3: One link, case **B**

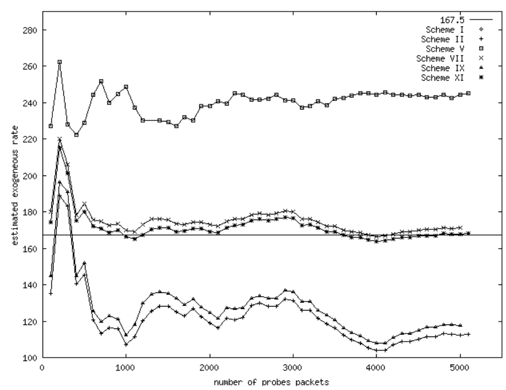

Figure 7.4: One link, case **C**

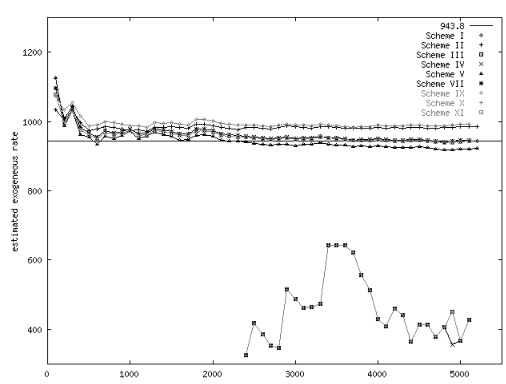

Figure 7.5: Two links, 1^{st} one is the bottleneck, case **A**

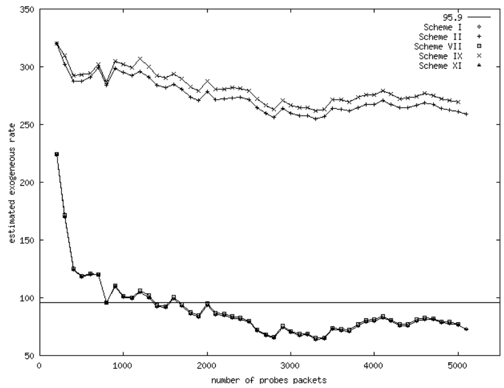

Figure 7.6: Two links, 1$^{\text{st}}$ one is the bottleneck, case **B**

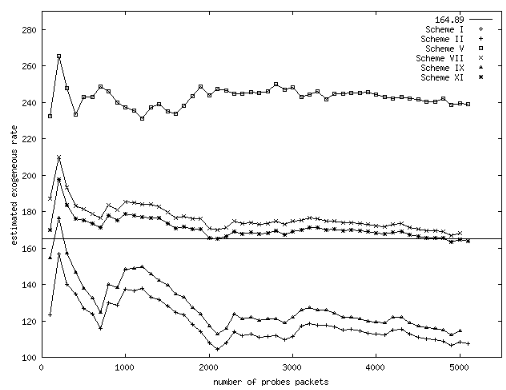

Figure 7.7: Two links, 1$^{\text{st}}$ one is the bottleneck, case **C**

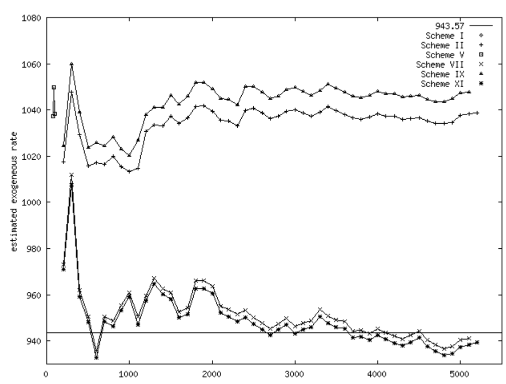

Figure 7.8: Two links, 2$^{\text{nd}}$ one is the bottleneck, case **A**

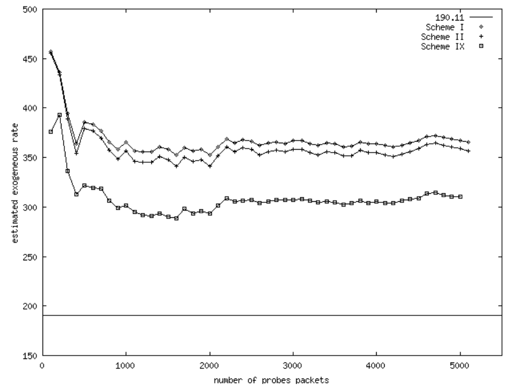

Figure 7.9: Two links, 2nd one is the bottleneck, case **C**

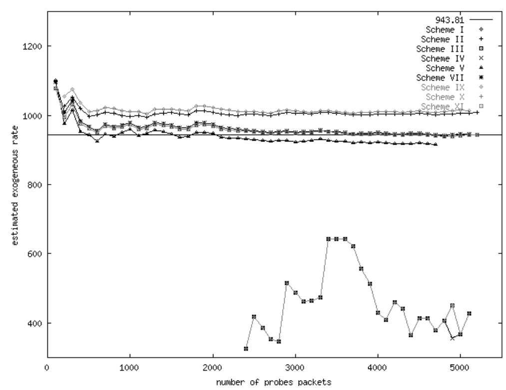

Figure 7.10: Three links, 1st one is the bottleneck, case **A**

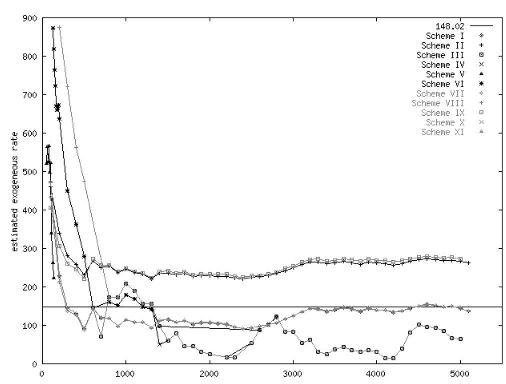

Figure 7.11: Three links, 1st one is the bottleneck, case **B**

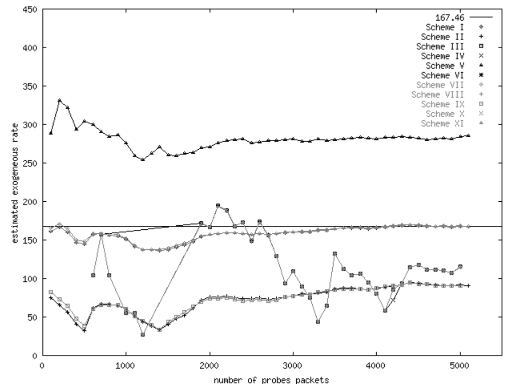

Figure 7.12: Three links, 1st one is the bottleneck, case **C**

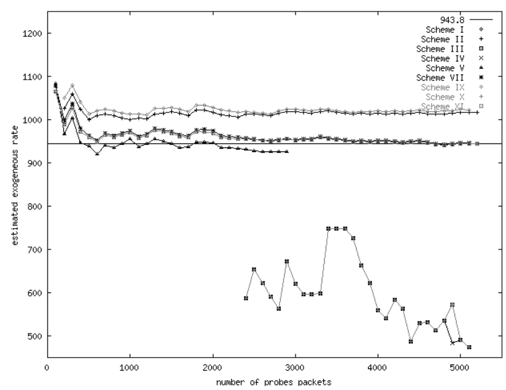

Figure 7.13: Three links, 2nd one is the bottleneck, case **A**

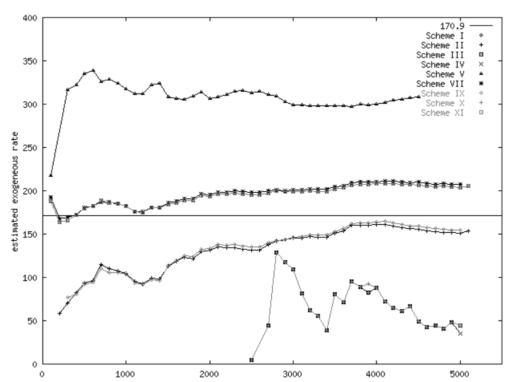

Figure 7.14: Three links, 2nd one is the bottleneck, case **C**

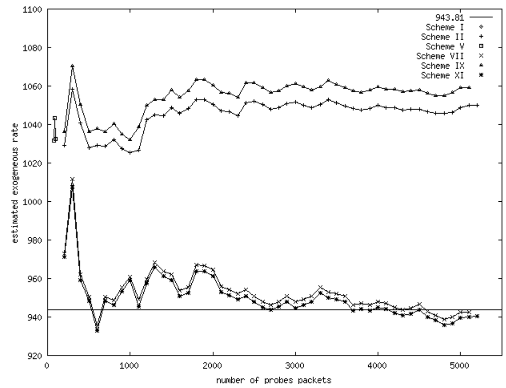

Figure 7.15: Three links, 3rd one is the bottleneck, case **A**

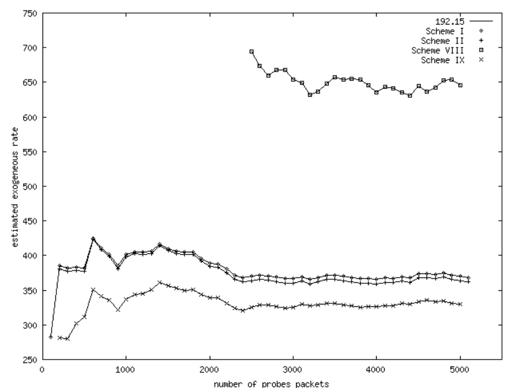

Figure 7.16: Three links, 3rd one is the bottleneck, case **C**

Buffer size versus number of probe packets

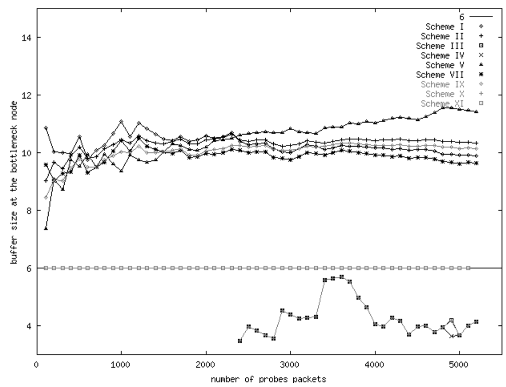

Figure 7.17: One link, case **A**

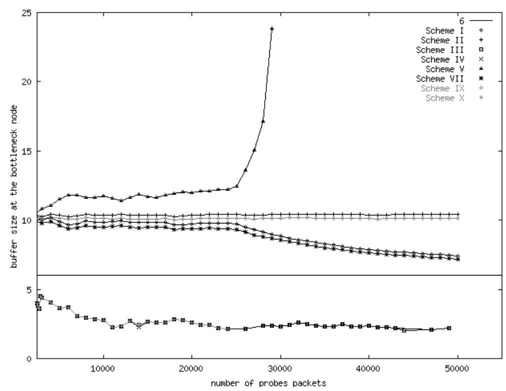

Figure 7.18: One link, case **A**, 50000 probe packets

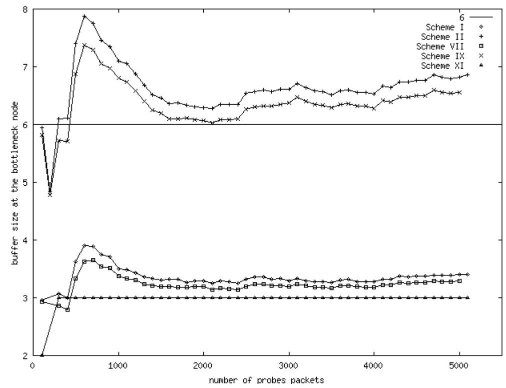

Figure 7.19: One link, case **B**

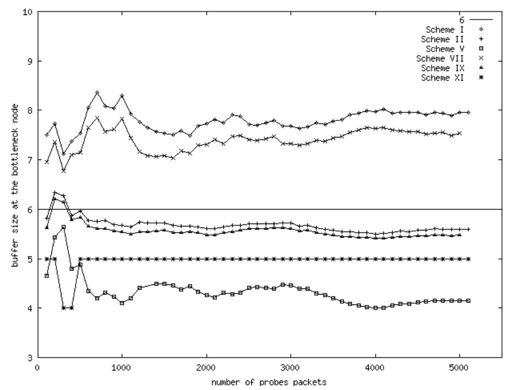

Figure 7.20: One link, case **C**

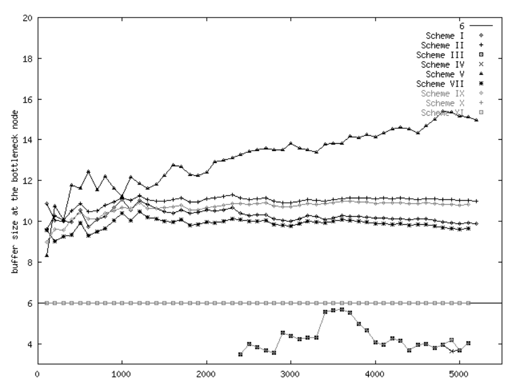

Figure 7.21: Two links, 1st one is the bottleneck, case **A**

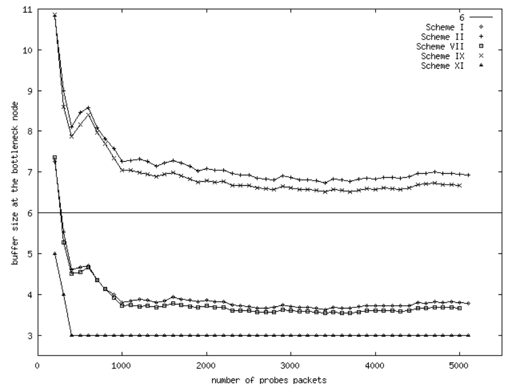

Figure 7.22: Two links, 1st one is the bottleneck, case **B**

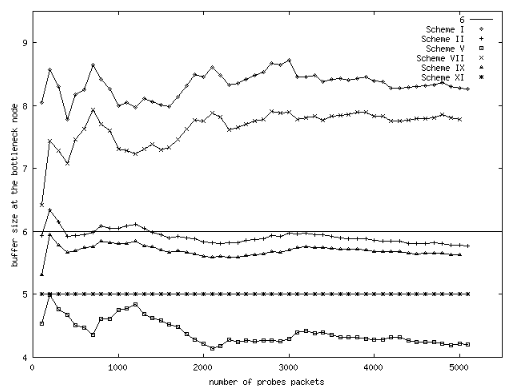

Figure 7.23: Two links, 1st one is the bottleneck, case **C**

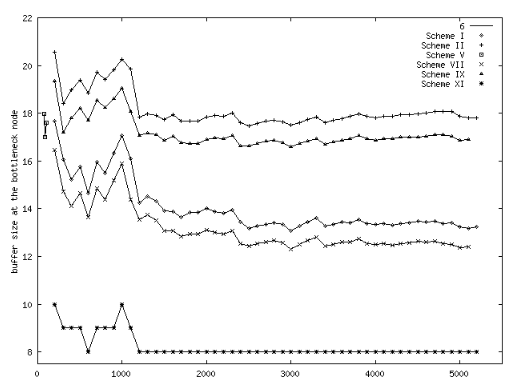

Figure 7.24: Two links, 2nd one is the bottleneck, case **A**

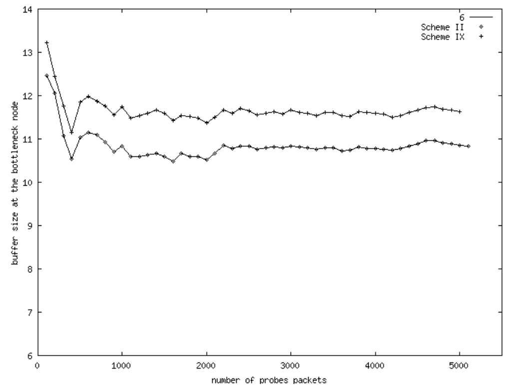

Figure 7.25: Two links, 2$^{\text{nd}}$ one is the bottleneck, case **C**

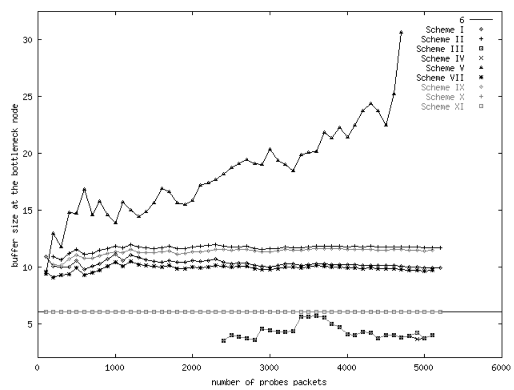

Figure 7.26: Three links, 1$^{\text{st}}$ one is the bottleneck, case **A**

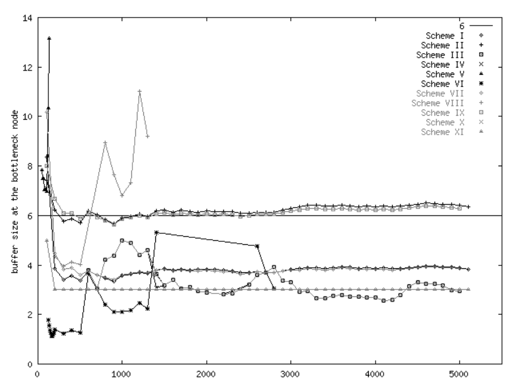

Figure 7.27: Three links, 1$^{\text{st}}$ one is the bottleneck, case **B**

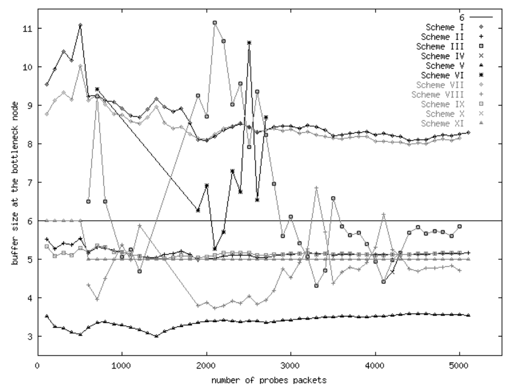

Figure 7.28: Three links, 1st one is the bottleneck, case **C**

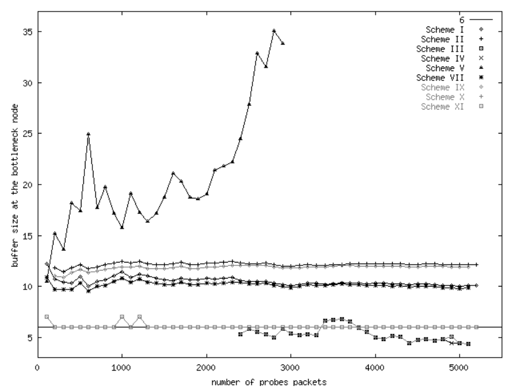

Figure 7.29: Three links, 2nd one is the bottleneck, case **A**

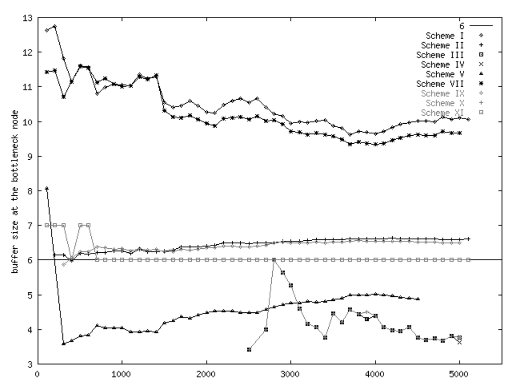

Figure 7.30: Three links, 2nd one is the bottleneck, case **C**

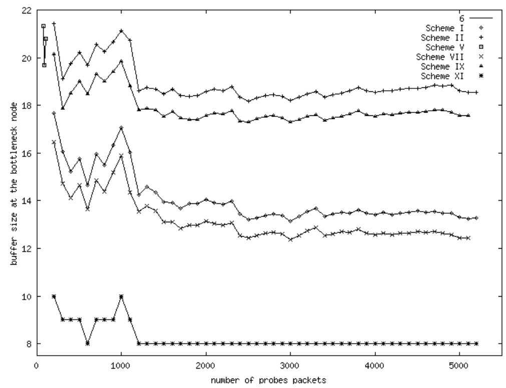

Figure 7.31: Three links, 3rd one is the bottleneck, case **A**

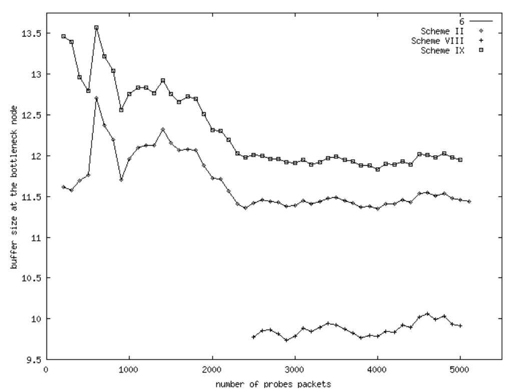

Figure 7.32: Three links, 3rd one is the bottleneck, case **C**